



Profiling the physiological pitfalls of anti-hepatitis C direct-acting agents in budding yeast

Galal Yahya^{1,2}  Nashwa Hashem Mohamed,³
Jordi Pijuan,⁴  Noura M. Seleem,¹ Rasha Mosbah,⁵
Steffen Hess,⁶ Ahmed A. Abdelmoaty,⁷ Rafa Almeer,⁸
Mohamed M. Abdel-Daim,^{8,9}
Hamoud Shulaywih Alshaman,¹⁰ Ibrahim Juraiby,¹¹
Kamel Metwally^{12,13} and Zuzana Storchova²

¹Department of Microbiology and Immunology, Faculty of Pharmacy, Zagazig University, Al Sharqia, 44519, Egypt.

²Department of Molecular Genetics, Faculty of Biology, Technical University of Kaiserslautern, Paul-Ehrlich Str. 24, Kaiserslautern, 67663, Germany.

³Hospitals of Zagazig University, Al Sharqia, Egypt.

⁴Laboratory of Neurogenetics and Molecular Medicine - IPER, Institut de Recerca Sant Joan de Déu, Barcelona, 08950, Spain.

⁵Infection Control Unit, Hospitals of Zagazig University, Al Sharqia, Egypt.

⁶Department of Cell Biology, Faculty of Biology, Technical University of Kaiserslautern, Kaiserslautern, Germany.

⁷Department of Tropical Medicine, Faculty of Medicine, Zagazig University, Zagazig, 44519, Egypt.

⁸Department of Zoology, College of Science, King Saud University, P.O. Box 2455, Riyadh, 11451, Saudi Arabia.

⁹Pharmacology Department, College of Veterinary Medicine, Suez Canal University, Ismailia, Egypt.

¹⁰Department of Urology, King Salman armed forces hospital, Tabuk, Saudi Arabia.

¹¹General Directorate of Health Affairs, Ministry of Health, Jazan, 82723, Saudi Arabia.

¹²Department of Pharmaceutical Chemistry, Faculty of Pharmacy, Tabuk University, Tabuk, 47713, Saudi Arabia.

¹³Department of Medicinal Chemistry, Faculty of Pharmacy, Zagazig University, Zagazig, 44519, Egypt.

treatment of chronic hepatitis C (CHC) virus infection as combination therapy with other antiviral medications. DAA-based therapy achieves high cure rates, reaching up to 97% depending on the genotype of the causative hepatitis C virus (HCV). While DAAs have been approved as an efficient and well-tolerated therapy for CHC, emerging concerns about adverse cardiac side effects, higher risk of recurrence and occurrence of hepatocellular carcinoma (HCC) and doubts of genotoxicity have been reported. In our study, we investigated in detail physiological off-targets of DAAs and dissected the effects of these drugs on cellular organelles using budding yeast, a unicellular eukaryotic organism. DAAs were found to disturb the architecture of the endoplasmic reticulum (ER) and the mitochondria, while showing no apparent genotoxicity or DNA damaging effect. Our study provides evidence that DAAs are not associated with genotoxicity and highlights the necessity for adjunctive antioxidant therapy to mitigate the adverse effects of DAAs on ER and mitochondria.

Introduction

Hepatitis C virus (HCV) is a liver-infecting RNA virus that belongs to the family Flaviviridae. Over 100 million people are chronically infected around the world, with the major complications of HCV infection being liver cirrhosis and emergence of hepatocellular carcinoma (Mohd Hanafiah *et al.*, 2013; Blach *et al.*, 2017). Egypt has the sharpest worldwide prevalence rates of HCV infection, with at least 15% of the population infected (Sievert *et al.*, 2011). Current guidelines recommend HCV treatment with direct-acting antivirals (DAAs)-based regimen for all HCV-infected patients, irrespective of the degree of liver fibrosis (World Health Organization, 2018). Sofosbuvir (SOF) is a novel nucleotide analogue prodrug that selectively inhibits the HCV non-structural protein 5B (NS5B), an RNA-dependent RNA polymerase crucial for the replication of HCV (Fung *et al.*, 2014). SOF is a component of the first oral, interferon (IFN)-free treatment authorized for a treatment of CHC infection (Asselah, 2014; Falade-Nwulia *et al.*, 2017). Daclatasvir (DCV) is one of the new DAAs that interfere with other stages of the HCV life cycle (Belema and Meanwell, 2014; Lim and Gallay, 2014). It is the first selective inhibitor of HCV non-structural protein

Summary

Sofosbuvir and Daclatasvir are among the direct-acting antiviral (DAA) medications prescribed for the

Received 15 January, 2021; revised 16 July, 2021; accepted 17 July, 2021.

For correspondence: E-mail gmetwa@bio.uni-kl.de; Tel. (+49) 631 205 5920; Fax: (+49) 631 205 4090. E-mail kametwally@hotmail.com; Tel. (+966) 14 427 3022; Fax: (+966) 14 427 3022.

Microbial Biotechnology (2021) 14(5), 2199–2213
doi:10.1111/1751-7915.13904

© 2021 The Authors. *Microbial Biotechnology* published by Society for Applied Microbiology and John Wiley & Sons Ltd.

This is an open access article under the terms of the Creative Commons Attribution-NonCommercial-NoDerivs License, which permits use and distribution in any medium, provided the original work is properly cited, the use is non-commercial and no modifications or adaptations are made.

5A (NS5A), and interference with this replication complex limits viral multiplication (Fung *et al.*, 2014; Degaspero *et al.*, 2015). The combination of both drugs with or without ribavirin provoked sustained virological response (SVR) in patients in different stages of advanced liver diseases (Sulkowski *et al.*, 2014; Wyles *et al.*, 2015; Moshyk *et al.*, 2016; Boglione *et al.*, 2017; Pol *et al.*, 2017).

Although DAAs initially showed significant promise when introduced to the market, subsequent studies noted a few limitations and deleterious side effects of these treatments. Therefore, a detailed investigations to explore interventions of DAAs with molecular pathways, cellular physiology and subcellular organelles are required (Maciocia *et al.*, 2016; Abouelkheir Abdalla *et al.*, 2017; Kim *et al.*, 2017; Andrade *et al.*, 2018; Hirose *et al.*, 2019; Kogiso *et al.*, 2019). Researchers were particularly concerned over the possible increase in incidence and relapse of HCC recorded in HCV patients after DAA therapy (Giovannini *et al.*, 2020; Lithy *et al.*, 2020; Muzica *et al.*, 2020; Pop *et al.*, 2020).

The budding yeast *Saccharomyces cerevisiae* is routinely used as a model organism to resolve biological pathways and evolutionary processes conserved between yeast and higher eukaryotes, and more recently as a platform to investigate newly synthesized therapeutics (Parsons *et al.*, 2006). The simple culture conditions and easy genetic manipulation of the yeast genome facilitate its extensive usage in various lines of biological research. Additionally, *S. cerevisiae* was the first unicellular eukaryote with a complete sequenced genome. The yeast genome has been completely sequenced since 1996 and comprises 6.275 genes organized on 16 chromosomes; the function of more than 92% of yeast genes has been identified (Botstein *et al.*, 1997). Comparative genomic analysis revealed that nearly 40% of yeast genes share conserved primary structure with at least one structural or functional homolog of human protein-coding genes (Parsons *et al.*, 2003). Moreover, 30% of human genes with identified function in genetic and pathological disorders have yeast orthologs (Foury, 1997). Due to this remarkable homology in the genome and the extreme conservation of basic cellular pathways, studies in yeast have facilitated the analysis of major cellular processes, such as mRNA translation and decay (Sonenberg *et al.*, 2000; Collier and Parker, 2004), DNA repair mechanisms (Tsukuda *et al.*, 2005) and the cell cycle regulation (Hartwell and Kastan, 1994). In this study, we used budding yeast for a detailed inspection of the adverse effects of DAAs on cell physiology, genome stability, and on subcellular organelles' architecture and integrity. Our chemical-genetic and organelle biology approach of our study revealed apparent effects on the dynamics of ER and mitochondria, while excluding any DNA damaging or genotoxic effects of DAAs.

Results

Susceptibility of budding yeast to SOF and DCV

We initially determined the minimum inhibitory concentration (MIC) of SOF (Fig. 1A) and DCV (Fig. 1B) in budding yeast cells. SOF and DCV were dissolved in DMSO, and twofold serial dilutions were prepared and added to the liquid culture of budding yeast adjusted to the same optical density. The effect of both drugs in different concentrations on growth and survival was monitored by reading the optical density after 16 h incubation. We found that the concentration of 64 μ M DCV was sufficient to inhibit the yeast growth compared with mock-treated control cells (Fig. 1C), whereas concentrations higher than 100 μ M of SOF were required to induce growth inhibition (Fig. 1D). These results indicate that DCV is less tolerated by budding yeast than SOF. In the same context, isogenic sets of polyploid yeast exhibited similar growth pattern to haploid strain when plated on plates containing inhibitory concentrations of each drug that were deduced from the growth curve of haploid yeast (Fig. 1E).

Exposure of budding yeast to DAAs perturbs cell volume

Perturbation of budding volume and morphology of budding yeast reflects several cellular stress signals and serves as an discernible phenotype of physiological aberrations, such as unfolded protein response (UPR), stress signals and cell cycle deregulations including cell cycle arrest and ageing (Scrimale *et al.*, 2009; Moreno *et al.*, 2019). Pathways that disturb cell volume are tightly linked to cell cycle progression, efficient protein folding machinery and DNA quality control pathways. Previously, fundamental regulators and genetic networks that control cell size in yeast and their homologs in mammalian cells were identified using systematic screens of yeast mutants that shift the size profile to smaller, or larger volume distributions (Jorgensen *et al.*, 2002; Zhang *et al.*, 2002; Ohya *et al.*, 2005; Dungrawala *et al.*, 2012; Soifer and Barkai, 2014; Yahya *et al.*, 2014). To explore the effect of SOF or DCV on budding yeast volume, we grew budding yeast in presence of sublethal doses of each drug and compared them with identical cultures grown with drugs known to induce ER stress (Dithiothreitol, DTT) (Hamdan *et al.*, 2017), UPR (Tunicamycin; TN) (Zhao *et al.*, 2019), and genotoxic stress (Hydroxyurea, HU) (Soriano-Carot *et al.*, 2012). As a control, we grew budding yeast with a vehicle of the tested drugs. Additionally, a yeast mutant (Δ *cln3*) (Yahya *et al.*, 2014) with a large cell volume due to a deletion of the G1 cyclin and another mutant (Δ *sfp1*) with a small budding volume due to a deletion of *SFP1*, the

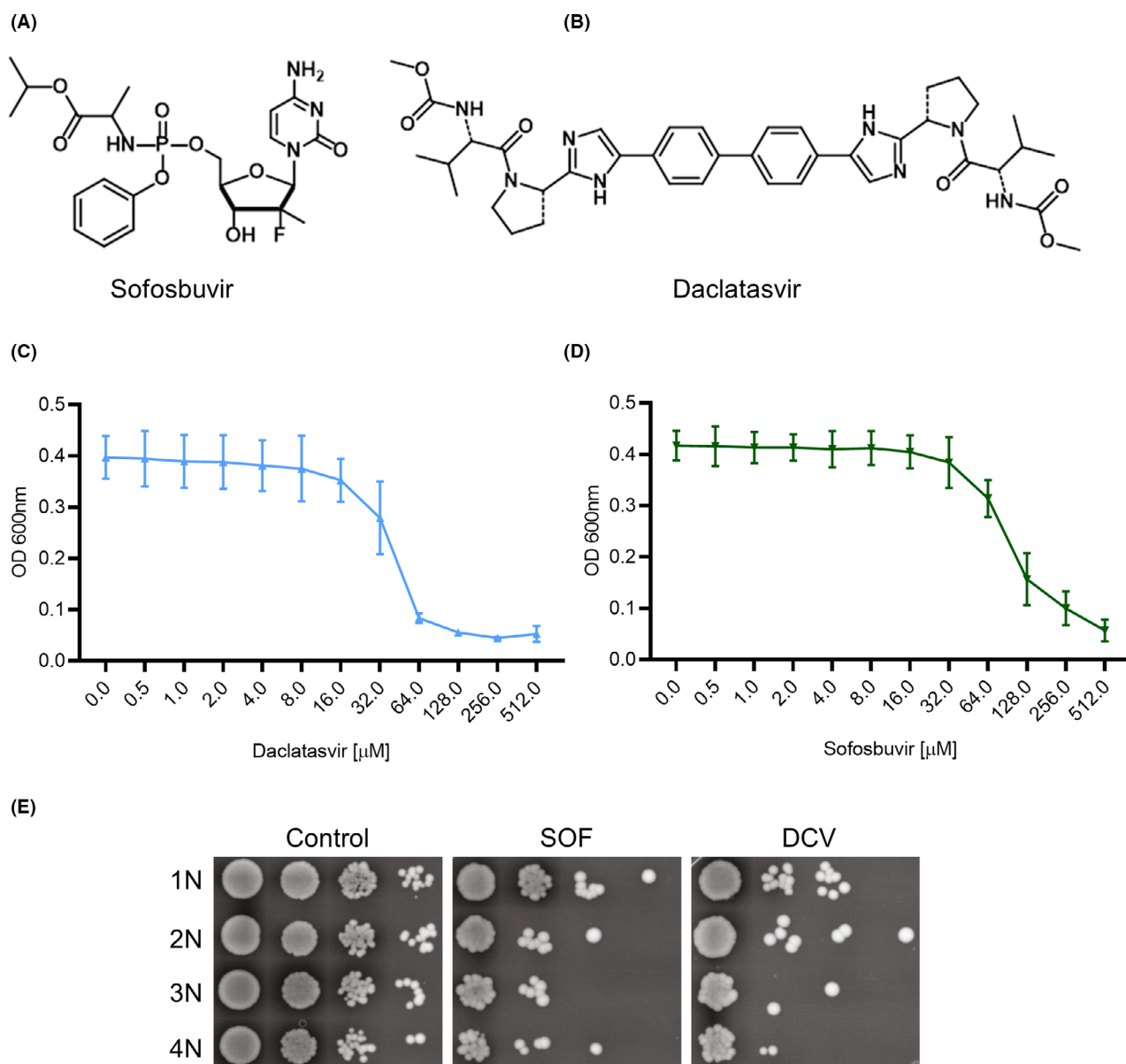


Fig. 1. Minimal inhibitory concentration (MIC) determination of Sofosbuvir and Daclatasvir. Chemical structures of (A) Sofosbuvir (SOF) and (B) Daclatasvir (DCV). (C) Dose–response curve of twofold serial dilutions of Daclatasvir (mean \pm SD; $n = 3$ independent biological replicates). (D) Dose–response curve of twofold serial dilutions of Sofosbuvir (mean \pm SD; $n = 3$ independent biological replicates). (E) Representative drop dilution of exponentially growing isogenic series of yeast strain of different ploidy on YPD plates supplemented with 128 μ M Sofosbuvir (SOF) or 64 μ M Daclatasvir (DCV). Plates were imaged after 48 h of incubation at 30 °C.

master transcription factor of ribosomal biogenesis, were analysed (Fig. 2A) (Sudbery, 2002; Cipollina *et al.*, 2008; Albert *et al.*, 2019). Budding yeast treated with DAAs showed significantly enlarged budding volume compared with control cells (CT (control): 48.87 ± 13.28 ; SOF: 71.3 ± 28.37 ($P < 0.0001$); DCV: 78.01 ± 34.17 ($P < 0.0001$)), although not as large as in cells treated with DTT (116.0 ± 34.83 ($P < 0.0001$)), TN (112.2 ± 34.80 ($P < 0.0001$)), HU (90.30 ± 31.13 ($P < 0.0001$)) or $\Delta cln3$ (100.7 ± 44.91 ($P < 0.0001$)),

while the control $\Delta sfp1$ showed the expected small volume (32.69 ± 12.36 ($P < 0.0001$)) (Fig. 2B). The prominent effects of DAAs on cell volume denote possible effects on cellular organelles and cell physiology.

DAAs disrupt the integrity and the morphology of ER

To further dissect the effects on cellular organelles and other physiological aspects that are affected by tested drugs, we investigated the effect of DAAs on ER

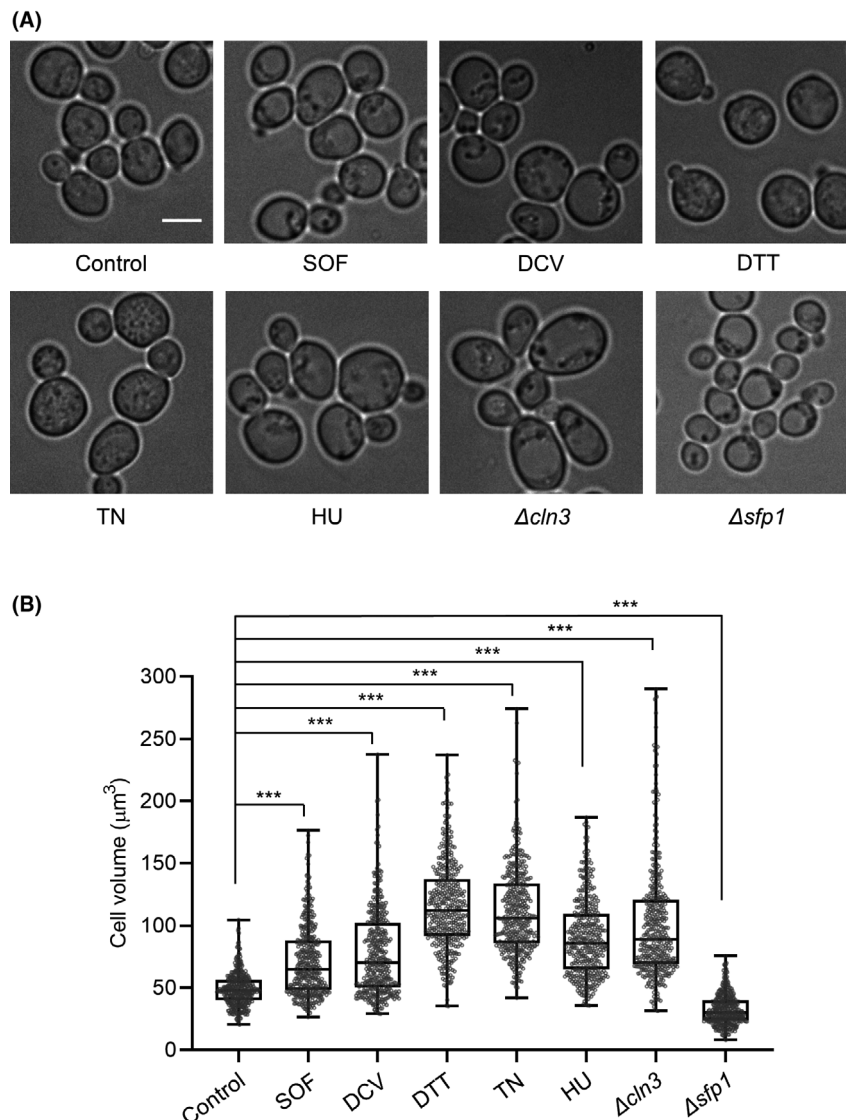


Fig. 2. Sofosbuvir and Daclatasvir enlarge budding volume.

A. Representative bright-field images of haploid yeast cell grown for 4–6 h in YPD media (control; CT), or media supplemented with 64 μM Sofosbuvir (SOF), 32 μM Daclatasvir (DCV), or other drugs that affect cell volume (5 mM Dithiothreitol; DTT, 5 μM Tunicamycin; TN and 200 mM Hydroxyurea; HU). $\Delta cln3$ mutant was used as a control for large cell volume and $\Delta sfp1$ for small cell volume. Scale bar: 5 μm .

B. Quantification of individual volumes at budding of (A) yeast cells (box plots represent 25th percentile, median, 75th percentile, the whiskers extend to the minimum and maximum values; $n = 400$ cells; 3 independent biological replicates). The statistical analysis was done using one-way ANOVA and Tukey–Kramer *post hoc* test (***) $P < 0.001$).

architecture. As a positive control, we used tunicamycin that is known to disturb ER integrity (Schuck *et al.*, 2009; Austriaco, 2012) in a background expressing Sec63-GFP, a subunit of the Sec62/Sec63 complex involved in post-translational translocation of proteins to ER and commonly employed to evaluate the ER integrity (Schuck *et al.*, 2009; Chaillot *et al.*, 2015). Sec63 is an essential ER translocation protein required for protein import to ER that localizes to both cortical ER (cER) and nuclear ER (nER). ER organization as judged microscopically by Sec63-GFP distribution and

compartmentalization was assessed in cells challenged with DAAs and in control cells. The control cells exhibited a clear and well-characterized ER organization with the nER around the nuclear compartment, the cER adjacent to plasma membrane at the cell periphery and few cytoplasmic ER tubes (Fig. 3A). However, in cells treated with tunicamycin, the ER became fragmented, and the GFP signal was diffused in the cytoplasm. The nER integrity was moderately or entirely disrupted in some cells (Fig. 3A). Cells treated with DAAs contained large cytoplasmic foci, possibly representing collapsed ER

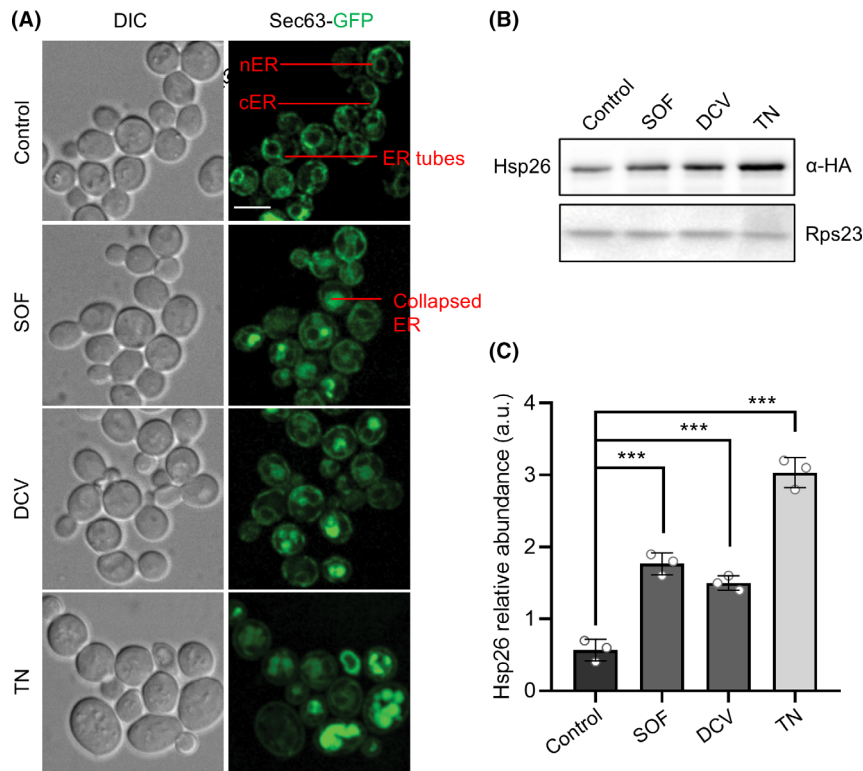


Fig. 3. Effect of Sofosbuvir and Daclatasvir on ER architecture.

A. Representative fluorescence images of Sec63-GFP localization in control cells (CT), cells treated with 64 μM Sofosbuvir (SOF), 32 μM Daclatasvir (DCV) or 5 μM Tunicamycin (TN) as a positive control for ER stressing agent for 4–6 h. Cortical (cER) and nuclear ERs (nER) are labelled. Scale bar, 5 μm .

B. Expression analysis of heat shock protein Hsp26. Cells expressing Hsp26-6HA were exponentially grown for 4–6 h in YPD media supplemented with DMSO, 64 μM Sofosbuvir (SOF), 32 μM Daclatasvir (DCV) or 5 μM Tunicamycin (TN). Levels of Hsp26-6HA were analysed by Western blot, and Rps23 was used as a loading control.

C. Relative abundance quantification of Hsp26-6HA in (B). Mean \pm SD (3 independent biological replicates). The statistical analysis was done using one-way ANOVA and Tukey–Kramer *post hoc* test (***) $P < 0.001$.

(Fig. 3A). Taken together, these findings indicate that DAAs disrupt ER organization. DAAs-treated cells also showed enhanced upregulation (relative to untreated cells) of Hsp26 (CT: 0.56 ± 0.15 ; SOF: 1.77 ± 0.15 ($P < 0.0001$); DCV: 1.50 ± 0.1 ($P < 0.0001$)), a small cytosolic heat shock protein (sHSP) with a molecular chaperone function (Petko and Lindquist, 1986; Carmelo and Sá-Correia, 1997), albeit to a lower level than in cells treated with TN (3.03 ± 0.20 ($P < 0.0001$)) (Fig. 3B and C). The altered ER morphology and upregulated markers of UPR response indicate that DAAs induce ER stress and accumulation of unfolded protein.

Yeasts treated with DAAs show no apparent genotoxicity

The major concerns about any new drug arise from possible mutagenic or genotoxic effects. To investigate possible genotoxic effects of DAAs, we monitored the phosphorylation status of Rad53, an essential protein kinase required for DNA damage signalling (Cordón-

Preciado *et al.*, 2006). Upon exposure to DNA damaging agent, Rad53p amplifies initial signals through modifying the phosphorylation state of downstream protein targets that recognize DNA damage and block replication (Allen *et al.*, 1994; Weinert *et al.*, 1994). Yeast cultures arrested in G1 by alpha factor were released into media with the tested drugs or a vehicle; as a positive control for DNA damage, we treated yeast culture with HU. Cells treated with HU showed a dramatic increase of Rad53 protein levels (2.00 ± 0.26 ($P < 0.0001$)) and noticeable shift to high phosphorylated forms, while yeasts cells treated with DAAs (SOF: 0.45 ± 0.12 ($P = \text{n.s.}$); DCV: 0.44 ± 0.14 ($P = \text{n.s.}$)) or the control (CT: 0.42 ± 0.22) show no change in the level or in the phosphorylation status of Rad53 (Fig. 4A and B); in the same experiment we monitored the budding index as an indicator of the cell cycle progression, cells treated with DAAs were able to pass G1, enter S phase and normally behave as control cells while HU-treated cells clearly arrested in S phase (Fig. 4C). Drugs that interfere with

microtubule dynamics and tubulin polymerization, for example benomyl, are highly genotoxic and lead to aneuploidy due to incorrect segregation of sister chromatids (Georgieva *et al.*, 1990; Mailhes and Aardema, 1992). A sensitive assay to record correct segregation was used, where segregation of chromosome 4 labelled by tetO/TetR-GFP system near centromeres was monitored in

cells released from mitotic arrest into media with or without the tested drugs (He *et al.*, 2000). Again, no significant changes were observed in cells treated with DAAs (SOF: 93.0 ± 2.64 ($P = \text{n.s.}$) and DCV: 92.0 ± 4.00 ($P = \text{n.s.}$)) compared with control cells (CT: 92.33 ± 3.05), while the benomyl treated cells showed clear signs of chromosomes mis-segregation (Benomyl:

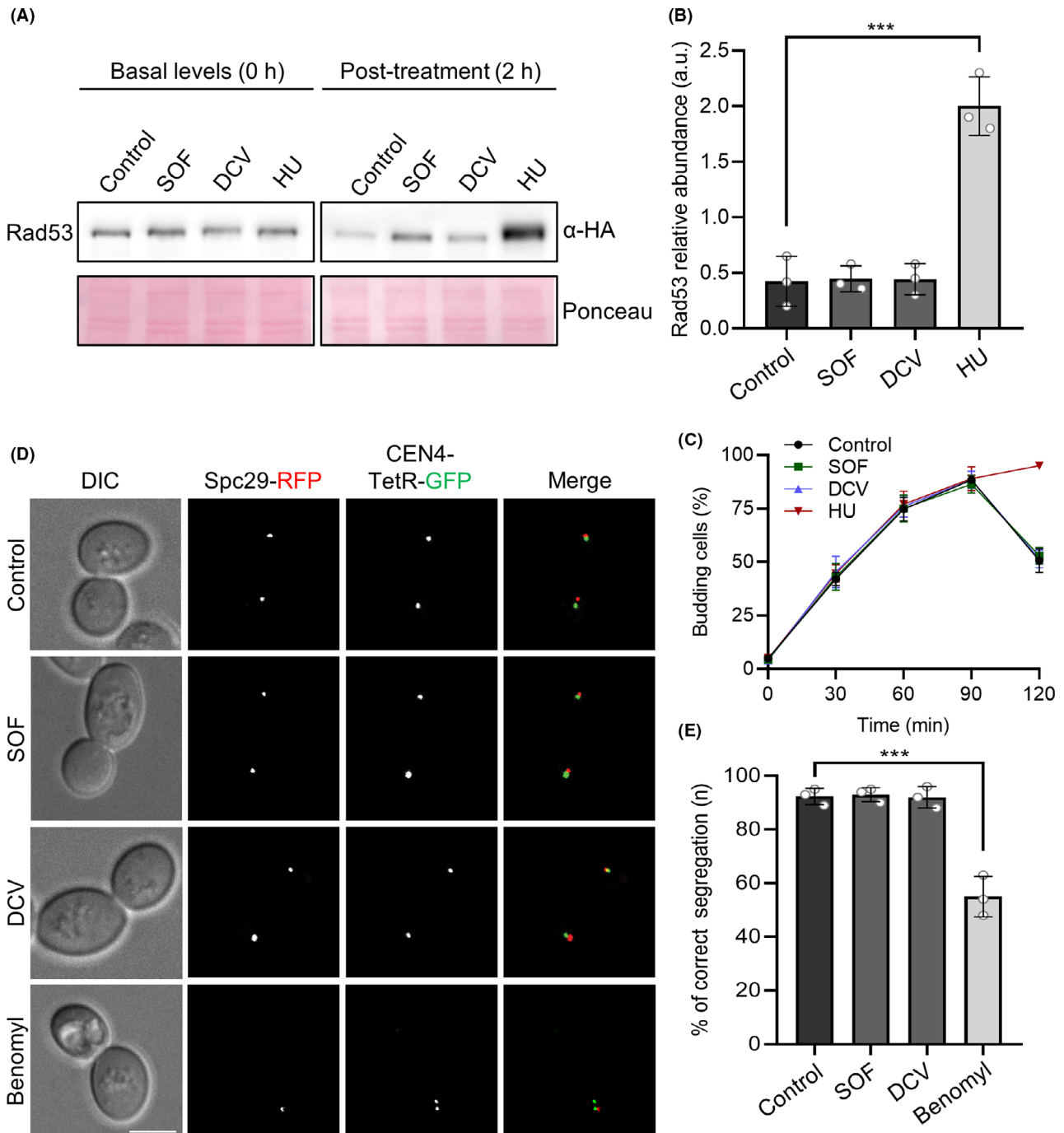


Fig. 4. Sofosbuvir and Daclatasvir cause no genotoxic stress.

55.0 ± 7.55 ($P < 0.0001$)) (Fig. 4D and E). Together, these results suggest no genotoxic effects of the DAAs.

DAAs reduce the integrity and quantity of mitochondrial DNA

To evaluate possible effects of DAAs on mitochondrial DNA, we stained DNA of live cells growing in the presence of DAAs with DAPI (Fig. 5A). Treated cells showed a decrease in the mitochondrial DNA. We quantified the mtDNA content relative to genomic DNA using qPCR with specific primers that target *COX3*, a gene encoded in the mitochondrial DNA and the housekeeping *ACT1* in the genomic DNA. As a control, we used a yeast *rho*⁰ strain lacking the mtDNA. The distribution of mtDNA was significantly altered after the treatment, as DAAs-treated cells showed a significant decrease of mtDNA compared with control cells (CT: 1.00 ± 0.0; SOF: 0.71 ± 0.01 ($P < 0.0001$); DCV: 0.74 ± 0.04 ($P < 0.0001$)) (Fig. 5B). Additionally, we evaluated mitochondrial Cox2 protein levels by Western blot and observed a significant decrease (SOF: 0.65 ± 0.01 ($P < 0.0001$); DCV: 0.76 ± 0.06 ($P < 0.0001$)) compared with control cells (CT: 1.54 ± 0.19, Fig. 5C and D)). As a negative control, we treated cells with chloramphenicol (CHL) that inhibits mitochondrial translation and thus reduced Cox2 protein levels (0.44 ± 0.09 ($P < 0.0001$)). These results show that DAAs reduced the levels and the integrity of mtDNA.

DAAs cause distinct mitochondrial fragmentation and impair mitochondrial respiration

Mitochondria are cellular organelles with a main function to generate energy. In addition to this role, mitochondria are involved in maintenance of calcium homeostasis, metabolism of amino acid and nucleotides, and biosynthesis of iron–sulphur clusters, haeme and ubiquinone (Young, 2017). Yeast strains that were cultured in growth

media supplemented with DAAs showed enhanced fragmentation of mitochondria similar to the pattern exhibited by yeast strain depleted of mitochondrial DNA, whereas control cultures exhibited the typical network morphology of mitochondria, when mitochondrial integrity was examined by microscopy (Fig. 6A). To test a direct effect of altered mitochondrial integrity and loss of mtDNA, we tested oxygen concentration is well-established indicator for mitochondrial function. Indeed, yeasts treated with DAAs showed significantly reduced oxygen concentration and lower basal respiration (Fig. 6B).

Discussion

DAAs display high performance and satisfactory safety profile in patients since their introduction into drug markets for the control of Hepatitis C. DAAs have dramatically changed the HCV treatment landscape, with elevated sustained virologic response (SVR), potential benefits in CHC treatment and improved compliance (Asselah, 2014; Virlogeux *et al.*, 2016; Shiha *et al.*, 2018; Heffernan *et al.*, 2019). DAAs-based therapy of HCV infections has achieved high virologic cure rates (>90%) superior to the interferon-based therapy [interferon (INF) plus ribavirin (RBV)], with a low SVR not exceeding 50% (Seo *et al.*, 2017). Common side effects of DAAs are fatigue, nausea, dizziness and anaemia. However, with the wide application of DAAs combination regimens, recent clinical studies indicated unwanted side effects and development of certain types of cancer, which raises concerns about possible effects of DAAs on genome stability and other aspects of cellular physiology.

DAAs display no signs of genotoxicity

Yeast-based screens have been well established for various chemical biology studies to monitor genotoxicity and cytotoxicity, identify DNA damaging agents, determine

A. Cells expressing Rad53-6HA were exponentially grown in YPD media, arrested in G1 phase with α -factor and then released into YPD media supplemented with DMSO, 64 μ M Sofosbuvir (SOF), 32 μ M Daclatasvir (DCV) or 200 mM Hydroxyurea (HU) as a positive control for genotoxic stress. Samples were collected at time 0 and after 2 h post-treatments. Basal levels and phosphorylation of Rad53-6HA were analysed by Western blot. Ponceau staining was used as a loading control.

B. Relative abundance quantification of Rad53-6HA (relative to time 0 before treatment) in (A). Mean ± SD (3 independent biological replicates). The statistical analysis was performed using one-way ANOVA and Tukey–Kramer *post hoc* test ($***P < 0.001$).

C. Budding index for the respective cells in (A), samples were collected at the indicated time points, budding index was calculated after microscopic examination (at least 200 cells per count were scored). Mean ± SD is shown from 3 independent biological replicates.

D. Chromosome segregation (centromeres of chromosome 4 labelled by CEN4-tetO/TetR-GFP; in green) in cells grown in media supplemented with DMSO, 64 μ M Sofosbuvir (SOF) 32 μ M Daclatasvir (DCV) or benomyl (10 μ g ml⁻¹). Spc29-RFP stains the spindle pole bodies; in red. Scale bar, 5 μ m.

E. Percentage (mean ± SD) of correct chromosome segregation of cells in (D); (correct segregation was identified as a distribution of the 2 chromatids between mother and daughter cells, while existence of two dots in one cell was scored as a mis-segregation event, at least $n = 300$ cells for each experiment were counted; 3 independent biological replicates). The statistical analysis was done using one-way ANOVA and Tukey–Kramer *post hoc* test ($***P < 0.001$).

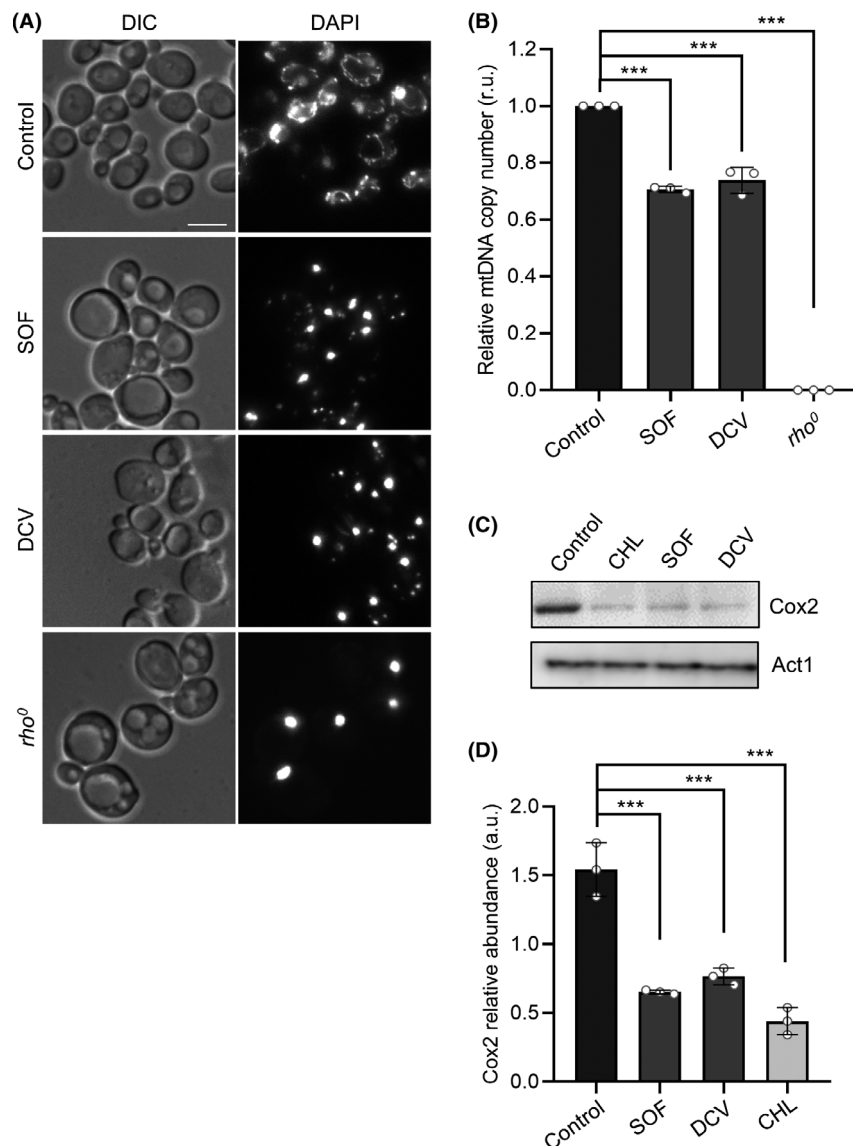


Fig. 5. Sofosbuvir and Daclatasvir affect integrity and copy number of mitochondrial DNA.

A. Mitochondrial nucleoid signals in control cells, 64 μ M Sofosbuvir (SOF), 32 μ M Daclatasvir (DCV) and cells depleted of mitochondrial DNA (*rho*⁰) as a negative control. Cells were grown to mid-logarithmic growth phase (6–8 h) in YPG media and stained with DAPI to visualize DNA. Scale bar, 5 μ m.

B. Quantification of mitochondrial DNA copy number by qPCR for the respective cells in (A). Total DNA was extracted from respective cells, and qPCR was performed using primers for *COX3* (mitochondrial DNA locus) and *ACT1* (housekeeping chromosomal DNA locus). Mean \pm SD ($n = 3$ independent biological replicates). The statistical analysis was done using one-way ANOVA and Tukey–Kramer *post hoc* test (** $P < 0.001$).

C. Cox2 protein levels analysed by Western blot in control cells, 64 μ M Sofosbuvir (SOF), 32 μ M Daclatasvir (DCV) or with 50 μ g ml⁻¹ Chloramphenicol (CHL) as a negative control.

D. Relative abundance quantification of Cox2 in (C). Mean \pm SD (3 independent biological replicates). The statistical analysis was done using one-way ANOVA and Tukey–Kramer *post hoc* test (** $P < 0.001$).

the underlying mechanisms and configure side effects of the newly synthesized drugs on functional organelles and metabolism (Kock *et al.*, 2009; dos Santos, 2012; van Bui *et al.*, 2015; Zhou *et al.*, 2016; Fasullo *et al.*, 2017; Delerue *et al.*, 2019). Polyploid yeast shows prominent sensitivity compared with haploid or diploid

yeasts when challenged with drugs and chemicals that induce genotoxicity or interfere with chromosome maintenance or organization, including DNA damaging and microtubule depolymerizing drugs (Storchová *et al.*, 2006; Yahya *et al.*, 2021). In case of DAAs, both haploid and polyploid yeasts exhibited similar sensitivity profile

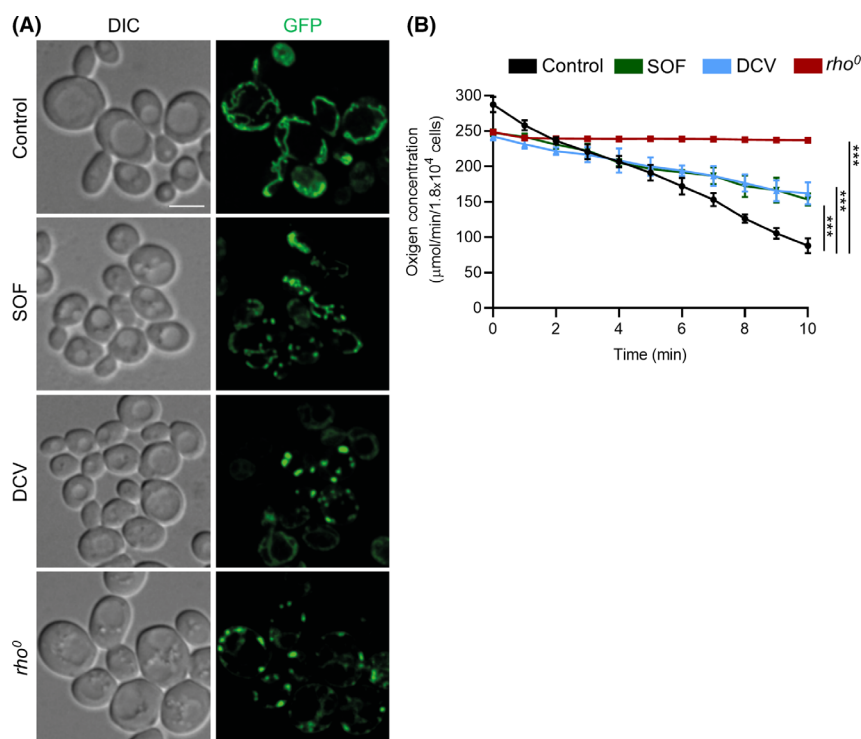


Fig. 6. Sofosbuvir and Daclatasvir alter mitochondria integrity and impair mitochondria respiration.

A. Representative fluorescence microscopy images of control cells, 64 μM Sofosbuvir (SOF) or 32 μM Daclatasvir (DCV) and respiratory deficient cells (ρho^0) as a negative control. Cells harbouring pYX232-mtGFP (a plasmid for expression of mitochondria-targeted GFP in yeast) were grown to mid-logarithmic growth phase (6–8 h) in YPG, and then subjected to fluorescent microscopy to visualize mitochondria. Scale bar, 5 μm .

B. Oxygen concentration of respective cells in (A). Values are mean oxygen concentration \pm SD ($n = 3$ independent biological replicates). The statistical analysis was performed using Kruskal–Wallis test followed by Dunn *post hoc* test (***) $P < 0.001$.

at the same inhibitory concentration of DAAs. Moreover, cells treated or untreated with DAAs displayed similar budding profile and segregated their duplicated chromosomes with the same efficiency. Additionally, DAAs-treated yeast did not accumulate high phosphorylated forms of Rad53, a well-known marker of genotoxic stress response. All these results suggest that DAAs treatment has negligible genotoxic effects.

DAAs disturb the architecture of ER and mitochondria

ER has been frequently reported as a nonspecific target of several antiviral agents (Ganta and Chaubey, 2019). Therefore, we tested the global effect of DAAs on organelles integrity. Indeed, yeast cells treated with DAAs showed discernible signature of ER disturbance in the form of fragmented or collapsed ER, accompanied with upregulation of cytosolic heat shock protein Hsp26, possibly in response to UPR provoked by ER stress.

Previous studies showed that the antiviral nucleoside analogues, such as zidovudine (AZT), can generate mitochondrial toxicity upon long-term treatment (Sun *et al.*, 2014; Jin *et al.*, 2017). Our study found that

mitochondria were strongly affected in response to DAAs. Treated cells suffered from alterations of mitochondrial dynamics, accumulated fractured mitochondria and showed distortion of the network pattern of healthy mitochondria. Moreover, DAAs-treated cells displayed significant loss of mtDNA. The exact role of DAAs in disturbing the mitochondrial physiology and organization has not been investigated in detail, although mitochondrial toxicity triggered by antiviral drugs and DAAs has been previously recognized (Lewis and Dalakas, 1995; Kakuda, 2000; Kim *et al.*, 2017). The undesirable effects of DAAs on mitochondrial morphology and the level of mtDNA likely caused the reduced oxygen consumption and lower basal respiration rate. Our observation may provide a mechanistic explanation for the clinical side effects that include fatigue and dizziness observed in most patients. In the same context, drugs that interfere with mitochondrial homeostasis were found to promote alterations of cardiac physiology (Varga and Pacher, 2018). Together with our findings, this may explain the reported cardiac toxicity associated with DAAs (Ucciferri *et al.*, 2017; El Missiri *et al.*, 2020).

DAA and hepatitis B reactivation

Due to pharmacological eradication of HCV, DAAs may possibly reactivate hepatitis B virus (HBV) in formerly infected patients. Thus, the European Medicines Agency (EMA) and the United States Food and Drug Administration (FDA) have recommended checking all HCV patients for HBV coinfection before starting DAA-based therapy for HCV to reduce the risk of HBV reactivation (Cheung *et al.*, 2016; Chen *et al.*, 2017; Holmes *et al.*, 2017; Loggi *et al.*, 2017; Blackard and Sherman, 2018; El Kassas *et al.*, 2018; Jiang *et al.*, 2018; Wang *et al.*, 2019; Miyasaka *et al.*, 2020; Palacios-Baena *et al.*, 2020). Our findings may present another indirect link between induction of ER stress and mitochondrial disturbance due to DAAs treatment and HBV reactivation, although this assumption will require further investigation. It was reported that HBV can induce ER stress and activate UPR. The HBV-induced ER stress and UPR signalling increase the folding capacity of the infected cells by upregulating chaperons as a response to the accumulated unfolded proteins. HBV can employ this folding protein surplus for processing viral proteins, genome replication or virion assembly (Lazar *et al.*, 2014). Additionally, the DAAs-induced ER stress may instigate stimuli sufficient for reactivating inactive HBV.

Experimental procedures

Strains, plasmids and growth conditions

Yeast strains and bacterial plasmids used in this study are listed in Table S1. Yeast strains were based on the W303 or S288C genetic backgrounds of a mating type (Winston *et al.*, 1995). Yeast-diluted precultures were grown exponentially for 4–5 generations in YP (1% yeast extract, 2% peptone), or in synthetic complete media (SC; 1.34% yeast nitrogen base, 0.04% complete synthetic mix) supplemented with 2% glucose (YPD or SDC), or 2% galactose (YPG or SGC), aerated by shaking at 30 °C. Yeast cells were arrested in late G1 by treating exponential cultures with 5 µg ml⁻¹ α-factor (Core Facility, Max Planck Institute of Biochemistry, Martinsried, Germany) for 105 min at 30 °C, or arrested in mitosis by adding 30 µg ml⁻¹ nocodazole for 3 h at 30 °C (Santa Cruz Biotechnology; Dallas, TX, USA).

General genetic methods

Standard protocols were used for DNA manipulations and transformation of yeast cells. Single null mutants and epitope fusion to target genes were constructed using the homologous recombination approach after PCR amplification of the antibiotic resistance kanMX4 cassettes with short homologous sequences flanking the

gene of interest and selection for geneticin resistance (Wach *et al.*, 1994; Janke *et al.*, 2004). Gene deletions were confirmed by PCR analysis. For adding the C-terminus epitope tags, Phusion DNA Polymerase (Thermo Fisher Scientific; Waltham, MA, USA) was used.

Determination of growth sensitivities

Sensitivity assays to DAAs were carried out by spotting 1:10 serial dilutions of exponential cultures onto YPD plates supplemented with the tested drugs at 30 °C for 48 h (Pijuan *et al.*, 2015).

Minimal inhibitory concentration (MIC) determination

A log phase culture in complete synthetic media was diluted to 0.02 OD₆₀₀ as determined in a standard spectrophotometer, in a sterile 96-well plate (Thermo Fisher Scientific) with rounded bottom. Tested drugs were diluted in the same medium (2-fold serial dilution) starting from a concentration of 512 µM. 100 µl of the diluted culture was added to 100 µl of diluted chemicals using a multichannel pipette and mixed three times (3 wells were mixed with a blank as a control and one well was free from cells and drug), then covered and incubated at 30 °C for 16 to 20 h with gentle shaking. Plates were then removed, and OD measurements were monitored using GloMax[®] Discover Microplate Reader (Promega; Madison, WI, USA).

Oxygen concentration analysis

Cells were grown exponentially in YPG medium. 125 µM DCV or 500 µM SOF was added, and the cultures were further grown for 6–8 h. 1 OD₆₀₀ cells were collected by centrifugation (5000 g, 5 min, room temperature) and resuspended in water. An Oxygraph (Hansatech Instruments; Pentney, UK) was calibrated with oxygen-saturated and oxygen-depleted water, using sodium dithionite for oxygen removal. Oxygen levels of 900 µl of saturated growth medium were measured until a plateau was reached, 100 µl of cell suspension was added and oxygen levels were measured continuously until they reached 0 µmol ml⁻¹.

Western blot analysis

Total cell lysate was prepared from cell pellets with 5 OD₆₀₀, where 15 µl of 5 M urea was added to cell pellet and boiled for 2 min immediately. An equal volume of glass beads was added, then cell suspensions were vortexed for 8 min at room temperature, and 50 µl of 2% SDS and 0.125 M Tris–HCl pH 6.8 were then added,

vortexed for 2 additional min, boiled for 2 min and centrifuged. The protein concentration was determined by the Micro DC protein assay (Bio-Rad, Richmond, CA, USA). Total protein was separated in polyacrylamide gel and blotted to PVDF membranes (GE Healthcare, Chicago, IL, USA). The membranes were blocked with 5% skim-milk and washed in TBS-0.1% Tween-20 buffer (25 mM Tris, 50 mM NaCl, 2.5 mM KCl and 0.1% Tween-20). Afterwards, the membranes were incubated with the specific primary antibodies overnight at 4 °C. After three washes, the membranes were incubated with the secondary antibody coupled to the horseradish peroxidase for 2 h at room temperature (Table S2). Membranes were incubated with Amersham ECL Prime Western Blotting Detection Reagent and visualized by iBright™ CL1000 Imaging System (Thermo Fisher Scientific). The intensity of individual bands was measured using ImageJ software (NIH, Bethesda, MD, USA; <http://rsb.info.nih.gov/ij>).

DNA isolation and mitochondrial quantitative PCR analysis

Total DNA was extracted using YeaStar™ Genomic DNA Kit (Zymo Research; Irvine, CA, USA) according to the manufacturer's instructions from mid-logarithmic growth cultures. Total DNA was subjected to qPCR using the iQ-Supremix (Bio-Rad). qPCR reactions were performed in 96-well plates with 20 µl of volume using Maxima™ SYBR Green qPCR Master Mix (Thermo Fisher Scientific) according to the manufacturer's instructions. For mtDNA and nuclear DNA, loci within the *COX3* and *ACT1* were amplified respectively (see Table S2 for primer sequences). mtDNA levels were calculated relative to nuclear DNA by the $2^{-\Delta\Delta CT}$ method (Livak and Schmittgen, 2001).

Immunofluorescence

Differential interference contrast (DIC) and fluorescence microscopy images were captured from living cells with AxioScope 2 microscope (Zeiss; Jena, Germany). Images were acquired with a Cool-SNAP-HQ 12-bit monochrome digital camera (Roper Scientific; Trenton, NJ, USA). Yeast cultures were grown exponentially in liquid growth medium (YPD or YPG) supplemented with the indicated drugs. Cell samples were collected and concentrated 10-fold by centrifugation (12 000 g, during 1 min at room temperature); then, cell suspensions were incubated with 1 µg ml⁻¹ 4',6-diamidino-2-phenylindole (DAPI) for 5 min to stain the DNA. More than 200 cells from at least three independent experiments were analysed in each measurement.

Miscellaneous

Cell volume was determined from bright-field images and measured by BudJ plugin (Ferrezuelo *et al.*, 2012) using ImageJ; budding index was calculated according to (Amponsah *et al.*, 2021). All chemical compounds used in this work are listed in Table S3.

Statistical analyses

Data are presented as mean ± standard deviation (SD) and box plots showing the median, box edges [25th–75th percentiles], and the whiskers prolonged to the minimum and maximum values. Statistical significance was assessed by application of the Kolmogorov–Smirnov normality test followed by one-way ANOVA and Tukey–Kramer post hoc test (parametric test), or Kruskal–Wallis test followed by Dunn post hoc test (non-parametric test). *P*-values are indicated by asterisks **P* < 0.05; ***P* < 0.01; ****P* < 0.001. All statistical tests were conducted using GraphPad Prism software v.8.0.2 (GraphPad; La Jolla, CA, USA).

Acknowledgements

G.Y. is grateful to the Alexander-von-Humboldt Foundation (AVH) for granting the Return Fellowship EGY 1194703 GF-P. R.A. and M.M.A. would like to extend their sincere appreciation to the Researchers Supporting Project number (RSP-2020/96), King Saud University, Riyadh, Saudi Arabia.

Conflict of interest

The authors declare that they have no conflict of interest.

Funding Information

G. Y. was funded by Return Fellowship EGY 1194703 GF-P awarded by the Alexander-von-Humboldt Foundation. J. P. was supported by 'Beques de Recerca IRSJD-Carmen de Torres 2020'. The funders had no role in study design, analysis or decision to publish.

References

- Abouelkheir Abdalla, D., Ali Elhadidy, T., Besheer, T., and Elsayed Farag, R. (2017) Respiratory adverse effects of Sofosbuvir-based regimens for treatment of chronic hepatitis C virus. *Egyptian J Chest Dis Tuberc* **66**: 363–367.
- Albert, B., Tomassetti, S., Gloor, Y., Dilg, D., Mattarocci, S., Kubik, S., *et al.* (2019) Sfp1 regulates transcriptional networks driving cell growth and division through multiple promoter-binding modes. *Genes Dev* **33**: 288–293.

- Allen, J.B., Zhou, Z., Siede, W., Friedberg, E.C., and Elledge, S.J. (1994) The SAD1/RAD53 protein kinase controls multiple checkpoints and DNA damage-induced transcription in yeast. *Genes Dev* **8**: 2401–2415.
- Amponsah, P.S., Yahya, G., Zimmermann, J., Mai, M., Mergel, S., Mühlhaus, T., et al. (2021) Peroxiredoxins couple metabolism and cell division in an ultradian cycle. *Nat Chem Biol* **17**: 477–484.
- Andrade, X.A., Paz, L.H., Nassar, M., Oramas, D.M., Fuentes, H.E., Kovarik, P., et al. (2018) Primary liver diffuse large B-cell lymphoma following complete response for hepatitis C infection after direct antiviral therapy. *Acta Haematol* **139**: 77–80.
- Asselah, T. (2014) Daclatasvir plus sofosbuvir for HCV infection: an oral combination therapy with high antiviral efficacy. *J Hepatol* **61**: 435–438.
- Austriaco, N. (2012) Endoplasmic reticulum involvement in yeast cell death. *Front Oncol* **2**: 87.
- Belema, M., and Meanwell, N.A. (2014) Discovery of daclatasvir, a pan-genotypic hepatitis C virus NS5A replication complex inhibitor with potent clinical effect. *J Med Chem* **57**: 5057–5071.
- Blach, S., Zeuzem, S., Manns, M., Altraif, I., Duberg, A.-S., Muljono, D.H., et al. (2017) Global prevalence and genotype distribution of hepatitis C virus infection in 2015: a modelling study. *Lancet Gastroenterol Hepatol* **2**: 161–176.
- Blackard, J.T., and Sherman, K.E. (2018) Hepatitis B virus (HBV) reactivation—the potential role of direct-acting agents for hepatitis C virus (HCV). *Rev Med Virol* **28**: e1984.
- Boglione, L., Pinna, S.M., Cardellino, C.S., de Nicolò, A., Cusato, J., Carcieri, C., et al. (2017) Treatment with daclatasvir and sofosbuvir for 24 weeks without ribavirin in cirrhotic patients who failed first-generation protease inhibitors. *Infection* **45**: 103–106.
- Botstein, D., Chervitz, S.A., and Cherry, J.M. (1997) Yeast as a model organism. *Science* **277**: 1259–1260.
- van Bui, N., Nguyen, T.T.H., Bettarel, Y., Nguyen, T.H.T., Pham, T.L., Hoang, T.Y., et al. (2015) Genotoxicity of chemical compounds identification and assessment by yeast cells transformed With GFP Reporter Constructs Regulated by the PLM2 or DIN7 Promoter. *Int J Toxicol* **34**: 31–43.
- Carmelo, V., and Sá-Correia, I. (1997) HySP26 gene transcription is strongly induced during *Saccharomyces cerevisiae* growth at low pH. *FEMS Microbiol Lett* **149**: 85–88.
- Chaillot, J., Tebbji, F., Remmal, A., Boone, C., Brown, G.W., Bellaoui, M., and Sellam, A. (2015) The monoterpene carvacrol generates endoplasmic reticulum stress in the pathogenic fungus *Candida albicans*. *Antimicrob Agents Chemother* **59**: 4584–4592.
- Chen, G., Wang, C., Chen, J., Ji, D., Wang, Y., Wu, V., et al. (2017) Hepatitis B reactivation in hepatitis B and C coinfecting patients treated with antiviral agents: a systematic review and meta-analysis. *Hepatology* **66**: 13–26.
- Cheung, M.C.M., Walker, A.J., Hudson, B.E., Verma, S., McLaughlan, J., Mutimer, D.J., et al. (2016) Outcomes after successful direct-acting antiviral therapy for patients with chronic hepatitis C and decompensated cirrhosis. *J Hepatol* **65**: 741–747.
- Cipollina, C., van den Brink, J., Daran-Lapujade, P., Pronk, J.T., Vai, M., and de Winde, J.H. (2008) Revisiting the role of yeast Sfp1 in ribosome biogenesis and cell size control: a chemostat study. *Microbiology* **154**(Pt 1): 337–346.
- Coller, J., and Parker, R. (2004) Eukaryotic mRNA decapping. *Annu Rev Biochem* **73**: 861–890.
- Cordón-Preciado, V., Ufano, S., and Bueno, A. (2006) Limiting amounts of budding yeast Rad53 S-phase checkpoint activity results in increased resistance to DNA alkylation damage. *Nucleic Acids Res* **34**: 5852–5862.
- Degasperi, E., Aghemo, A., and Colombo, M. (2015) Daclatasvir for the treatment of chronic hepatitis C. *Expert Opin Pharmacother* **16**: 2679–2688.
- Delerue, T., Tribouillard-Tanvier, D., Daloyau, M., Khosrobakhsh, F., Emorine, L.J., Friocourt, G., et al. (2019) A yeast-based screening assay identifies repurposed drugs that suppress mitochondrial fusion and mtDNA maintenance defects. *Dis Models Mech* **12**: dmm036558.
- Dungrawala, H., Hua, H., Wright, J., Abraham, L., Kasemsri, T., McDowell, A., et al. (2012) Identification of new cell size control genes in *S. cerevisiae*. *Cell Div* **7**: 24.
- El Kassas, M., Shimakawa, Y., Ali-Eldin, Z., Funk, A.-L., Wifi, M.N., Zaky, S., et al. (2018) Risk of hepatitis B virus reactivation with direct-acting antivirals against hepatitis C virus: a cohort study from Egypt and meta-analysis of published data. *Liver Int* **38**: 2159–2169.
- El Missiri, A.M., Rayan, M.M., Awad, M.M., and El Desoky, A.I. (2020) Assessing the impact of a combination of sofosbuvir and daclatasvir treatment for hepatitis C virus infection on heart rate, rhythm and heart rate variability using 24-hour ECG monitoring. *Egypt Heart J* **72**: 37–44.
- Falade-Nwulia, O., Suarez-Cuervo, C., Nelson, D.R., Fried, M.W., Segal, J.B., and Sulkowski, M.S. (2017) Oral direct-acting agent therapy for hepatitis C virus infection: a systematic review. *Ann Intern Med* **166**: 637–648.
- Fasullo, M., Freedland, J., St John, N., Cera, C., Egner, P., Hartog, M., and Ding, X. (2017) An in vitro system for measuring genotoxicity mediated by human CYP3A4 in *Saccharomyces cerevisiae*. *Environ Mol Mutagen* **58**: 217–227.
- Ferrezuelo, F., Colomina, N., Palmisano, A., Garí, E., Gallego, C., Csikász-Nagy, A., and Aldea, M. (2012) The critical size is set at a single-cell level by growth rate to attain homeostasis and adaptation. *Nat Commun* **3**: 1012.
- Foury, F. (1997) Human genetic diseases: a cross-talk between man and yeast. *Gene* **195**: 1–10.
- Fung, A., Jin, Z., Dyatkina, N., Wang, G., Beigelman, L., and Deval, J. (2014) Efficiency of incorporation and chain termination determines the inhibition potency of 2'-modified nucleotide analogs against hepatitis C virus polymerase. *Antimicrob Agents Chemother* **58**: 3636–3645.
- Ganta, K.K., and Chaubey, B. (2019) Endoplasmic reticulum stress leads to mitochondria-mediated apoptosis in cells treated with anti-HIV protease inhibitor ritonavir. *Cell Biol Toxicol* **35**: 189–204.
- Georgieva, V., Vachkova, R., Tzoneva, M., Kappas, A., and Morgan, W.F. (1990) Genotoxic activity of benomyl in different test systems. *Environ Mol Mutagen* **16**: 32–36.
- Giovannini, C., Fornari, F., Indio, V., Trerè, D., Renzulli, M., Vasuri, F., et al. (2020) Direct antiviral treatments for

- hepatitis C virus have off-target effects of oncologic relevance in hepatocellular carcinoma. *Cancers (Basel)* **12**: 2674.
- Hamdan, N., Kritsiligkou, P., and Grant, C.M. (2017) ER stress causes widespread protein aggregation and prion formation. *J Cell Biol* **216**: 2295–2304.
- Hartwell, L.H., and Kastan, M.B. (1994) Cell cycle control and cancer. *Science* **266**: 1821–1828.
- He, X., Asthana, S., and Sorger, P.K. (2000) Transient sister chromatid separation and elastic deformation of chromosomes during mitosis in budding yeast. *Cell* **101**: 763–775.
- Heffernan, A., Cooke, G.S., Nayagam, S., Thursz, M., and Hallett, T.B. (2019) Scaling up prevention and treatment towards the elimination of hepatitis C: a global mathematical model. *Lancet* **393**: 1319–1329.
- Hirose, S., Yamaji, Y., Tsuruya, K., Ogawa, Y., Miyaoka, M., and Kagawa, T. (2019) Rapid regression of B-cell non-Hodgkin's lymphoma after eradication of hepatitis C virus by direct antiviral agents. *Case Rep Gastroenterol* **13**: 336–341.
- Holmes, J.A., Yu, M.-L., and Chung, R.T. (2017) Hepatitis B reactivation during or after direct acting antiviral therapy - implication for susceptible individuals. *Expert Opin Drug Saf* **16**: 651–672.
- Janke, C., Magiera, M.M., Rathfelder, N., Taxis, C., Reber, S., Maekawa, H., *et al.* (2004) A versatile toolbox for PCR-based tagging of yeast genes: new fluorescent proteins, more markers and promoter substitution cassettes. *Yeast* **21**: 947–962.
- Jiang, X.-W., Ye, J.-Z., Li, Y.-T., and Li, L.-J. (2018) Hepatitis B reactivation in patients receiving direct-acting antiviral therapy or interferon-based therapy for hepatitis C: a systematic review and meta-analysis. *World J Gastroenterol* **24**: 3181–3191.
- Jin, Z., Kinkade, A., Behera, I., Chaudhuri, S., Tucker, K., Dyatkina, N., *et al.* (2017) Structure-activity relationship analysis of mitochondrial toxicity caused by antiviral ribonucleoside analogs. *Antiviral Res* **143**: 151–161.
- Jorgensen, P., Nishikawa, J.L., Breikreutz, B.-J., and Tyers, M. (2002) Systematic identification of pathways that couple cell growth and division in yeast. *Science* **297**: 395–400.
- Kakuda, T.N. (2000) Pharmacology of nucleoside and nucleotide reverse transcriptase inhibitor-induced mitochondrial toxicity. *Clin Ther* **22**: 685–708.
- Kim, S.-J., Jang, J.Y., Kim, E.-J., Cho, E.K., Ahn, D.-G., Kim, C., *et al.* (2017) Ginsenoside Rg3 restores hepatitis C virus-induced aberrant mitochondrial dynamics and inhibits virus propagation. *Hepatology* **66**: 758–771.
- Kock, J.L.F., Swart, C.W., Ncango, D.M., Munnik, I.A., Maartens, M.M.J., Pohl, C.H., and van Wyk, P.W.J. (2009) Development of a yeast bio-assay to screen anti-mitochondrial drugs. *Curr Drug Discov Technol* **6**: 186–191.
- Kogiso, T., Sagawa, T., Kodama, K., Tani, M., Katagiri, S., Egawa, H., *et al.* (2019) Hepatocellular carcinoma after direct-acting antiviral drug treatment in patients with hepatitis C virus. *JGH Open* **3**: 52–60.
- Lazar, C., Uta, M., and Branza-Nichita, N. (2014) Modulation of the unfolded protein response by the human hepatitis B virus. *Front Microbiol* **5**: 433.
- Lewis, W., and Dalakas, M.C. (1995) Mitochondrial toxicity of antiviral drugs. *Nat Med* **1**: 417–422.
- Lim, P.J., and Galloway, P.A. (2014) Hepatitis C NS5A protein: two drug targets within the same protein with different mechanisms of resistance. *Curr Opin Virol* **8**: 30–37.
- Lithy, R.M., Elbaz, T., H. Abdelmaksoud, A., M. Nabil, M., Rashed, N., Omran, D., *et al.* (2020) Survival and recurrence rates of hepatocellular carcinoma after treatment of chronic hepatitis C using direct acting antivirals. *Eur J Gastroenterol Hepatol*. <https://doi.org/10.1097/MEG.0000000000001972>.
- Livak, K.J., and Schmittgen, T.D. (2001) Analysis of relative gene expression data using real-time quantitative PCR and the 2⁻(-Delta Delta C(T)) Method. *Methods* **25**: 402–408.
- Loggi, E., Gitto, S., Galli, S., Minichiello, M., Conti, F., Grandini, E., *et al.* (2017) Hepatitis B virus reactivation among hepatitis C patients treated with direct-acting antiviral therapies in routine clinical practice. *J Clin Virol* **93**: 66–70.
- Maciocia, N., O'Brien, A., and Ardeshta, K. (2016) Remission of follicular lymphoma after treatment for hepatitis C virus infection. *N Engl J Med* **375**: 1699–1701.
- Mailhes, J.B., and Aardema, M.J. (1992) Benomyl-induced aneuploidy in mouse oocytes. *Mutagenesis* **7**: 303–309.
- Miyasaka, A., Yoshida, Y., Suzuki, A., Masuda, T., Okamoto, H., and Takikawa, Y. (2020) Hepatitis B virus reactivation after successful treatment of hepatitis C virus with sofosbuvir and ribavirin: a case report and literature review. *Medicine (Baltimore)* **99**: e22650.
- Mohd Hanafiah, K., Groeger, J., Flaxman, A.D., and Wiersma, S.T. (2013) Global epidemiology of hepatitis C virus infection: new estimates of age-specific antibody to HCV seroprevalence. *Hepatology* **57**: 1333–1342.
- Moreno, D.F., Parisi, E., Yahya, G., Vaggi, F., Csikász-Nagy, A., and Aldea, M. (2019) Competition in the chaperone-client network subordinates cell-cycle entry to growth and stress. *Life Sci Alliance* **2**: e201800277.
- Moshyk, A., Martel, M.-J., Tahami Monfared, A.A., and Goeree, R. (2016) Cost-effectiveness of daclatasvir plus sofosbuvir-based regimen for treatment of hepatitis C virus genotype 3 infection in Canada. *J Med Econ* **19**: 181–192.
- Muzica, C.M., Stanciu, C., Huiban, L., Singeap, A.-M., Sfarti, C., Zenovia, S., *et al.* (2020) Hepatocellular carcinoma after direct-acting antiviral hepatitis C virus therapy: a debate near the end. *World J Gastroenterol* **26**: 6770–6781.
- Ohya, Y., Sese, J., Yukawa, M., Sano, F., Nakatani, Y., Saito, T.I., *et al.* (2005) High-dimensional and large-scale phenotyping of yeast mutants. *Proc Natl Acad Sci USA* **102**: 19015–19020.
- Palacios-Baena, Z.R., Paniagua-García, M., López-Hernández, I., Fernández-Cuenca, F., and Ríos-Villegas, M.J. (2020) High risk of hepatitis B virus reactivation among patients treated with direct-acting antivirals and coinfecting with HCV and HIV. *J Infect* **80**: 469–496.
- Parsons, A.B., Geyer, R., Hughes, T.R., and Boone, C. (2003) Yeast genomics and proteomics in drug discovery and target validation. *Prog Cell Cycle Res* **5**: 159–166.
- Parsons, A.B., Lopez, A., Givoni, I.E., Williams, D.E., Gray, C.A., Porter, J., *et al.* (2006) Exploring the mode-of-action

- of bioactive compounds by chemical-genetic profiling in yeast. *Cell* **126**: 611–625.
- Petko, L., and Lindquist, S. (1986) Hsp26 is not required for growth at high temperatures, nor for thermotolerance, spore development, or germination. *Cell* **45**: 885–894.
- Pijuan, J., María, C., Herrero, E., and Bellí, G. (2015) Impaired mitochondrial Fe-S cluster biogenesis activates the DNA damage response through different signaling mediators. *J Cell Sci* **128**: 4653–4665.
- Pol, S., Bourliere, M., Lucier, S., Hezode, C., Dorival, C., Larrey, D., et al. (2017) Safety and efficacy of daclatasvir-sofosbuvir in HCV genotype 1-mono-infected patients. *J Hepatol* **66**: 39–47.
- Pop, C.S., Preda, C.M., Manuc, M., Gheorghe, L.S., Istratescu, D., Chifulescu, A.E., et al. (2020) Occurrence and recurrence of hepatocellular carcinoma in patients with HCV genotype 1b related cirrhosis treated with Ledipasvir+Sofosbuvir±Ribavirin. *J Gastrointest Liver Dis* **29**: 690–691.
- dos Santos, S.C. (2012) Yeast toxicogenomics: genome-wide responses to chemical stresses with impact in environmental health, pharmacology, and biotechnology. *Front. Gene.* **3**: 1–17.
- Schuck, S., Prinz, W.A., Thorn, K.S., Voss, C., and Walter, P. (2009) Membrane expansion alleviates endoplasmic reticulum stress independently of the unfolded protein response. *J Cell Biol* **187**: 525–536.
- Scrimale, T., Didone, L., de Mesy Bentley, K.L., and Krysan, D.J. (2009) The unfolded protein response is induced by the cell wall integrity mitogen-activated protein kinase signaling cascade and is required for cell wall integrity in *Saccharomyces cerevisiae*. *Mol Biol Cell* **20**: 164–175.
- Seo, K., Kim, S.K., Kim, S.R., Ohtani, A., Kobayashi, M., Kato, A., et al. (2017) Comparison of Sofosbuvir Plus ribavirin treatment with pegylated interferon plus ribavirin treatment for chronic hepatitis C genotype 2. *Dig Dis* **35**: 541–547.
- Shiha, G., Soliman, R., ElBasiony, M., Hassan, A.A., and Mikhail, N.N.H. (2018) Sofosbuvir plus Daclatasvir with or without ribavirin for treatment of chronic HCV genotype 4 patients: real-life experience. *Hepatol Int* **12**: 339–347.
- Sievert, W., Altraif, I., Razavi, H.A., Abdo, A., Ahmed, E.A., AlOmair, A., et al. (2011) A systematic review of hepatitis C virus epidemiology in Asia, Australia and Egypt. *Liver Int* **31(Suppl 2)**: 61–80.
- Soifer, I., and Barkai, N. (2014) Systematic identification of cell size regulators in budding yeast. *Mol Syst Biol* **10**: 761.
- Sonenberg, N., Hershey, J.W.B., and Mathews, M. (2000) *Translational control of gene expression*. Cold Spring Harbor, NY, USA: Cold Spring Harbor Laboratory Press.
- Soriano-Carot, M., Bañó, M.C., and Igual, J.C. (2012) The yeast mitogen-activated protein kinase Sit2 is involved in the cellular response to genotoxic stress. *Cell Div* **7**: 1.
- Storchová, Z., Breneman, A., Cande, J., Dunn, J., Burbank, K., O'Toole, E., and Pellman, D. (2006) Genome-wide genetic analysis of polyploidy in yeast. *Nature* **443(7111)**: 541–547.
- Sudbery, P. (2002) Cell biology. When wee meets whi. *Science* **297(5580)**: 351–352.
- Sulkowski, M.S., Gardiner, D.F., Rodriguez-Torres, M., Reddy, K.R., Hassanein, T., Jacobson, I., et al. (2014) Daclatasvir plus sofosbuvir for previously treated or untreated chronic HCV infection. *N Engl J Med* **370**: 211–221.
- Sun, R., Eriksson, S., and Wang, L. (2014) Zidovudine induces downregulation of mitochondrial deoxynucleoside kinases: implications for mitochondrial toxicity of antiviral nucleoside analogs. *Antimicrob Agents Chemother* **58**: 6758–6766.
- Tsukuda, T., Fleming, A.B., Nickoloff, J.A., and Osley, M.A. (2005) Chromatin remodelling at a DNA double-strand break site in *Saccharomyces cerevisiae*. *Nature* **438(7066)**: 379–383.
- Ucciferri, C., Occhionero, A., Vecchiet, J., and Falasca, K. (2017) Cardiac toxicity associated with HCV direct antiviral agents. *Mediterr J Hematol Infect Dis* **10**: e2018069.
- Varga, Z.V., and Pacher, P. (2018) Cardiotoxicity of drugs. In *Mitochondrial dysfunction caused by drugs and environmental toxicants*. Will, Y., and Dykens, J.A. (eds). Hoboken, NJ, USA: John Wiley & Sons, pp. 93–110.
- Virlogeux, V., Choupeaux, L., Pradat, P., Maynard, M., Bailly, F., Scholtès, C., et al. (2016) Sofosbuvir plus daclatasvir with or without ribavirin for chronic hepatitis C infection: impact of drug concentration on viral load decay. *Dig Liver Dis* **48**: 1351–1356.
- Wach, A., Brachat, A., Pöhlmann, R., and Philippsen, P. (1994) New heterologous modules for classical or PCR-based gene disruptions in *Saccharomyces cerevisiae*. *Yeast* **10**: 1793–1808.
- Wang, J., Hu, C., Chen, Y.i., Liu, Z., Yu, Q., Yang, S., et al. (2019) HBV reactivation during direct-acting antiviral therapy in hepatitis B and C coinfecting patients undergoing haemodialysis. *Antivir Ther* **24**: 77–84.
- Weinert, T.A., Kiser, G.L., and Hartwell, L.H. (1994) Mitotic checkpoint genes in budding yeast and the dependence of mitosis on DNA replication and repair. *Genes Dev* **8**: 652–665.
- Winston, F., Dollard, C., and Ricupero-Hovasse, S.L. (1995) Construction of a set of convenient *Saccharomyces cerevisiae* strains that are isogenic to S288C. *Yeast* **11**: 53–55.
- World Health Organization (2018) *Guidelines for the care and treatment of persons diagnosed with chronic hepatitis C virus infection*. Geneva, Switzerland: World Health Organization.
- Wyles, D.L., Ruane, P.J., Sulkowski, M.S., Dieterich, D., Luetkemeyer, A., Morgan, T.R., et al. (2015) Daclatasvir plus Sofosbuvir for HCV in patients coinfecting with HIV-1. *N Engl J Med* **373**: 714–725.
- Yahya, G., Menges, P., Ngandiri, D.A., Schulz, D., Wallek, A., Kulak, N., et al. (2021) *Scaling of cellular proteome with ploidy*.
- Yahya, G., Parisi, E., Flores, A., Gallego, C., and Aldea, M. (2014) A Whi7-anchored loop controls the G1 Cdk-cyclin complex at start. *Mol Cell* **53**: 115–126.
- Young, M.J. (2017) Off-target effects of drugs that disrupt human mitochondrial DNA maintenance. *Front Mol Biosci* **4**: 74.
- Zhang, J., Schneider, C., Ottmers, L., Rodriguez, R., Day, A., Markwardt, J., and Schneider, B.L. (2002) Genomic scale mutant hunt identifies cell size homeostasis genes in *S. cerevisiae*. *Curr Biol* **12**: 1992–2001.

- Zhao, W., Cui, H.-J., Qiu, K.-P., Zhou, T., Hong, X.-S., and Liu, X.-G. (2019) Yeast molecular chaperone gene SSB2 is involved in the endoplasmic reticulum stress response. *Anton Leeuw* **112**: 589–598.
- Zhou, C., Elia, A.E.H., Naylor, M.L., Dephoure, N., Ballif, B.A., Goel, G., *et al.* (2016) Profiling DNA damage-induced phosphorylation in budding yeast reveals diverse signaling networks. *Proc Natl Acad Sci USA* **113**: E3667–E3675.

Supporting information

Additional supporting information may be found online in the Supporting Information section at the end of the article.

Table S1. Yeast strains and plasmids used in this study.

Table S2. Sequences of PCR primer sets, and antibodies used in this study.

Table S3. Chemical compounds used in this study.